The influence of acceptor anneal temperature on the performance of InGaN/GaN quantum well light-emitting diodes

J. D. Thomson, I. A. Pope, P. M. Smowton, P. Blood, R. J. Lynch, G. Hill, T. Wang, and P. Parbrook

Citation: Journal of Applied Physics **99**, 024507 (2006); doi: 10.1063/1.2165405
View online: http://dx.doi.org/10.1063/1.2165405
View Table of Contents: http://scitation.aip.org/content/aip/journal/jap/99/2?ver=pdfcov
Published by the AIP Publishing

The influence of acceptor anneal temperature on the performance of InGaN/GaN quantum well light-emitting diodes

J. D. Thomson,[a] I. A. Pope, P. M. Smowton, and P. Blood
School of Physics and Astronomy, Cardiff University, Cardiff, Wales CF24 3YB, United Kingdom

R. J. Lynch, G. Hill, T. Wang, and P. Parbrook
Department of Electronic and Electrical Engineering, University of Sheffield, Mappin Street, Sheffield S1 3JD, United Kingdom

(Received 19 August 2005; accepted 13 December 2005; published online 30 January 2006)

Temperature-dependent measurements of the pulsed light-current characteristics of InGaN light-emitting diodes that were thermally annealed at different temperatures have been investigated. A distinct light output, at a fixed current density, with operating temperature arises where the light output increases as the operating temperature is reduced from 300 K, reaches a maximum, and then decreases with subsequent reductions of the operating temperature. We observe that light-emitting diodes thermally annealed at higher temperatures, which is believed to increase the number of electrically activated acceptors in the *p* layers, have a lower light output below 300 K and the maximum light output shifts to higher operating temperatures. Measured absorption and emission spectra show that the thermal anneal process has not affected the structure of the quantum wells within these samples. The light output, for a fixed current density, has been simulated as a function of operating temperature, and we find that by changing the concentration of acceptor atoms, compensating donor atoms, and the hole mobility in the *p* layers, the trends observed experimentally can be reproduced. On the basis of the simulations we find that the distinct behavior of the light output with operating temperature is due to the combination of Shockley-Reed-Hall recombination, at operating temperatures around 300 K, and electron drift leakage, at operating temperature below 300 K, and the increase of the acceptor concentration results in an increased electron drift leakage due to the change of the concomitant hole mobility. The simulations support the view that the experimental observations can be explained through changes of the acceptor concentration in the *p* layers when the thermal anneal temperature is increased. © *2006 American Institute of Physics*. [DOI: 10.1063/1.2165405]

I. INTRODUCTION

Optoelectronic devices fabricated with GaN-based materials are of technological importance as emitters and detectors over the entire visible wavelength range and deep into the ultraviolet. The advances in the growth techniques of GaN and the alloys with In and Al, along with the successful *p* doping of GaN, have been the major steps making the production of lasers and light-emitting diodes (LEDs) possible.

To achieve successful *p* doping of GaN, magnesium (Mg) atoms are generally used as the *p*-type dopant. However, the acceptor atom is usually electrically inactive after growth as hydrogen (H) can form a complex with the acceptor atom during the postgrowth cooling process.[1] Therefore, the Mg atom has to go through two processes to produce holes in the material. The first is electrical activation of the Mg acceptor atom in the lattice to create an acceptor and the second is the normal thermal ionization process, where the operating temperature and acceptor ionization energy lead to a fraction of the acceptors being ionized to produce free holes. Electrical activation of Mg can be achieved through a number of methods: low-energy electron-beam irradiation,[2] thermal annealing in nitrogen above 600 °C,[3–5] more recently thermal annealing with oxygen,[6] and the use of laser irradiation to induce activation.[7] Through these methods the Mg–H complex is broken and the Mg forms an electrically active acceptor, though the H can form a compensating donor if not completely removed.[8,9] However, the larger increase of the acceptor concentration compared to the compensating donor concentration results in an overall increase in hole concentration. These postgrowth steps can dramatically reduce the resistivity[1–4] and increase the hole concentration in the layer compared to as-grown Mg–GaN (Refs. 4–7) and are critical steps in the production of efficient LEDs and lasers. Through the analysis of Hall-effect measurements, where the temperature-dependent carrier concentration is measured, the acceptor and donor concentrations and the acceptor ionization energy can be determined. Postgrowth steps such as the examples above are usually required when the growth process involves H and temperatures above 1000 K are used, as is common in metal-organic vapor-phase epitaxy (MOVPE), whereas molecular-beam epitaxy (MBE) growth of Mg–GaN occurs below 1000 K and H is absent, producing electrically active *p*-type GaN without the need for postgrowth steps.[10]

The postgrowth step of thermal annealing in nitrogen is an established and widely used method of activating the Mg atoms in the *p* layers grown by MOVPE. In this work we

[a]Electronic mail: thomsonjd@cardiff.ac.uk

have experimentally investigated the effect of the thermal anneal temperature on the optical performance of MOVPE-grown InGaN multiple quantum well (MQW) LEDs through measurement of the light-current (LI) characteristics as a function of temperature and the absorption and emission spectra. We demonstrate that the thermal anneal temperature can affect the temperature dependence of the LI characteristics even though no noticeable change of the absorption spectrum of the InGaN quantum wells (QWs) is detected. We have used the device simulator[11] SIMWINDOWS to simulate device operation and to find that by changing the number of activated acceptors and compensating donors present in the *p*-doped layers and the concomitant hole mobility we can produce similar behaviors for the temperature dependence of the light output as those found experimentally. Analysis of the simulated results provides us with evidence that carrier loss from the QWs is significant in GaN-based LEDs and is dependent upon the acceptor concentration and hole mobility, giving further evidence that the conditions of the thermal anneal step can affect device performance.

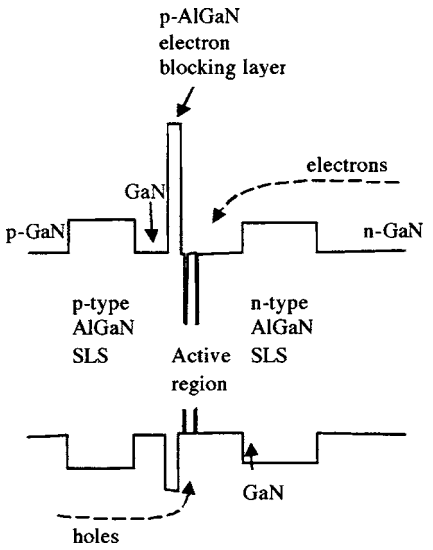

FIG. 1. Schematic band diagram of InGaN/GaN QW LED structure, where the AlGaN superlattice is represented as a bulk material with an average composition of 9% and the ten InGaN QWs within the active region are represented by two QWs.

II. EXPERIMENTAL METHODS AND RESULTS

The sample investigated was initially designed for laser studies and was fabricated into LED devices for this work. The structure was grown by MOVPE on a sapphire substrate. After a nucleation layer, 2 μm of nominally undoped GaN and 4 μm of *n*-type Si–GaN were grown, followed by 2 μm of highly doped Si–GaN. A 650 nm *n*-doped superlattice structure which consisted of 125 pairs of $Al_{0.18}Ga_{0.70}N$–GaN was grown followed by 150 nm of undoped GaN, the InGaN–GaN active region, 150 nm of undoped GaN, a 625 nm *p*-doped superlattice structure consisting of 125 pairs of $Al_{0.18}Ga_{0.70}N$–GaN, and then capped by a 300 nm *p*-doped Mg–GaN layer. The active region consisted of ten 2.5 nm $In_{0.10}Ga_{0.90}N$ QWs embedded between 7.5 nm GaN barriers and was followed immediately with a 20 nm *p*-doped $Mg–Al_{0.30}Ga_{0.70}N$ electron-blocking layer. The growth temperature of the *p*-type layers was 1220 K. Figure 1 shows a schematic band diagram of this InGaN/GaN MQW LED structure.

After growth four pieces of the sample were annealed individually at temperatures of 700, 750, 850, and 900 °C in a thermal annealer for 20 min in nitrogen prior to the fabrication into LEDs. The LEDs were fabricated together under the same conditions, and each had an emitting area of 2×10^{-8} m^2 and produced emission at 415 nm under electrical bias. The LI and emission characteristics of the LEDs were measured using pulsed electrical injection; a pulse length of 500 ns with a pulse rate of 1 kHz was used, giving a duty cycle of 0.05%, to reduce the self-heating effects that occur in continuous-wave operation.

The pulsed LI characteristics were measured as a function of operating temperature for each sample; the LI results for a LED from the sample annealed at 900 °C are shown in Fig. 2. The LI characteristics display a slight superlinear behavior for all temperatures investigated, which was also observed for the LED samples annealed at lower temperatures. An LED in which all the recombination was radiative would exhibit a linear LI characteristic and so the superlinearity suggests that a nonradiative recombination mechanism, which has a weaker dependence on carrier density than radiative recombination, is present in these samples. Unlike this work, in previous reports on InGaN LEDs, sublinear LI curves have been measured[12–14] and Pope *et al.*[14] have shown that drift-diffusion leakage from the QW produces the sublinear behavior and that the drift rate is dependent upon the electrical properties of the *p*-type GaN cap layer. Despite the different shape of the LI curves for the samples in this paper, we will show that drift-diffusion leakage cannot be ignored and that the superlinear shape of the LI characteristic is due to a combination of radiative, Shockley-Reed-Hall, and drift-diffusion leakage current.

At a fixed current density, for example, as indicated by the dashed line in Fig. 2, the light output increases with operating temperature from 260 to 280 K where it reaches a maximum and then decreases with subsequent increases in the operating temperature up to 340 K. This distinct behavior of the light output with operating temperature has been reported previously by other groups for other InGaN–GaN

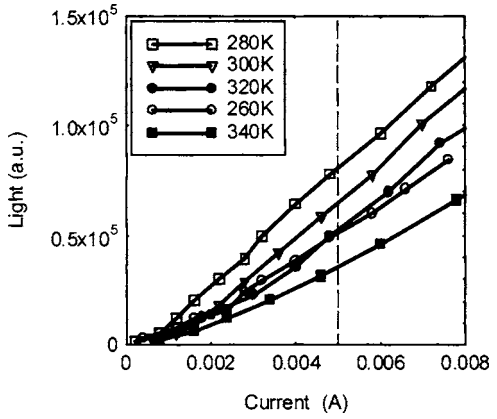

FIG. 2. Light-current curves for an LED annealed at 900 °C.

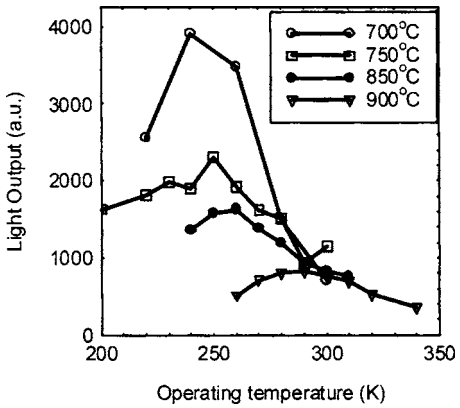

FIG. 3. Light output at a fixed current density (25 A cm^{-2}) vs temperature for the LEDs annealed at temperatures of 700, 750, 850, and 900 °C.

LEDs.[12–14] The distinct behavior, shown in Fig. 2 for the sample annealed at 900 °C, was also observed in the LED samples annealed at lower temperatures. The values of the light output for a fixed current density of 25 A cm^{-2} are shown in Fig. 3 for all anneal temperatures. At operating temperatures around 300 K, Fig. 3 indicates no significant difference in the light output between LEDs from samples annealed at different temperatures unlike the results reported by Youn *et al.*[15] where the electroluminescence at 20 mA decreases with increasing thermal anneal temperature and is attributed to "large fluctuations in the In content or phase segregation" in the QWs during annealing. In our study, as the operating temperature is lowered below 300 K, the light output for all four LED samples increases (before decreasing again at still lower temperatures). In addition the sample annealed at 700 °C has the highest increase in the light output while the sample annealed at 900 °C has the lowest increase. The maximum light output from the LED annealed at 900 °C is about four times less than the maximum light output achieved from the LED annealed at 700 °C. Additionally the operating temperature at which the maximum light output occurs differs for the LED samples where the LEDs annealed at 700 °C have a maximum light output at 240 K while the LEDs annealed at 900 °C have a maximum light output at 290 K.

The absorption spectrum of each LED has been measured using edge photovoltage absorption spectroscopy.[16] Figure 4(a) shows the measured absorption spectra for the four LED samples and are typical of InGaN QWs, where the absorption increases slowly with increasing energy.[14] The absorption spectra (of the InGaN QWs) obtained from all four LEDs are similar, suggesting that the different thermal anneal temperatures have not caused any detectable differences between the LED samples. Previous studies have shown that intermixing of the InGaN QWs and GaN barriers can occur during thermal annealing.[17–21] Our absorption results imply that any intermixing of the InGaN QW and GaN barriers within these structures has not occurred over the range of anneal temperatures (700–900 °C) used in this study. Our results are consistent with previous studies where a thermal anneal temperature of 900 °C was not sufficient to cause any structural changes within the active region. Chuo *et al.*[18] reported that thermal annealing at 900 °C produces photoluminescence (PL) similar to as-grown samples and that when higher thermal anneal temperatures are used a blueshift of the PL is detected as a result of intermixing, while the work of McCluskey *et al.*[21] shows that it is not until a thermal anneal temperature above 1200 °C is used that a blueshift is detected in the spontaneous emission. The electroluminescent emission spectra of the LEDs annealed at different temperatures are shown in Fig. 4(b) for a current density of 20 A cm^{-2}, from which there is no discernable evidence that the different thermal anneal temperatures used have caused any change in the InGaN QWs. The wavelength at which the peak intensity occurs does differ slightly between the LEDs though the full widths half maximum (FWHMs) of the spectra are similar with value of FWHM=18 nm. The LED sample annealed at 850 °C emits at shorter wavelengths while the LED sample annealed at 900 °C emits at longer wavelengths. The other two samples emit at wavelengths in between these two; therefore there is no pattern to link the behavior of the emission with the anneal temperature of the samples. We suspect that the small differences observed in the emission spectra are due to small differences in the carrier density in each well and the resultant effect of band filling and screening of the piezoelectric field.[22] As described later the carrier density in the wells can be different even though the current densities are the same and so the small differences in the emission spectra are not evidence of any change in the quantum wells themselves. In summary, there is no evidence from the absorption and emission measurements that the active region has been affected by the different thermal anneal temperatures.

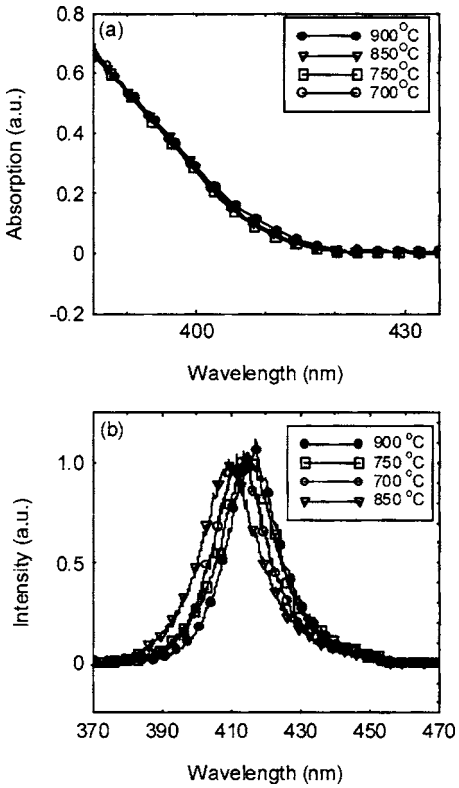

FIG. 4. (a) Photovoltage absorption of the InGaN QWs and (b) electroluminescence spectra at 25 A cm^{-2} for the LEDs annealed at temperatures of 700, 750, 850, and 900 °C.

TABLE I. Parameters common to the three structures used in the simulation.

Parameter	Value
Electron mass	$0.2m_o$
Heavy-hole mass	$1.6m_o$
Light-hole mass	$1.6m_o$
Spin-orbit mass	$0.17m_o$
QW radiative recombination coefficient ($cm^2\ s^{-1}$)	3×10^{-8}
QW nonradiative lifetime (ns)	1.5
Barrier nonradiative lifetime (ns)	0.5
Electron mobility ($cm^2\ V^{-1}\ s^{-1}$)	900
GaN band gap (eV)	3.4
Valence-band offset	0.67

III. SIMULATION

To understand what cause the different behaviors in the LI characteristics with operating temperature, we have simulated how the light output varies with operating temperature for InGaN LED structures. If we assume that the effect of postgrowth annealing is to vary the acceptor and donor concentrations in the material, we can explore the effects of annealing by modeling the operation of the device for different dopant concentrations. We have used the device simulator[11] SIMWINDOWS which is a one-dimensional drift-diffusion simulator which solves electrical, optical, and thermal equations for a described structure and was developed and successfully used to analyze vertical cavity surface-emitting lasers (VCSELs).[23] The simulator includes Fermi statistics and incomplete ionization of the dopants. To simplify the structure the AlGaN superlattice is treated as a continuous AlGaN layer with an average Al composition of 9% as shown in Fig. 1. The parameters which are common to the three structures are given in Table I, while in the following sections we discuss the critical aspects of our analysis.

The temperature dependences of the hole concentration and of the hole mobility are important in this study as they are both affected by the change of acceptor concentration. Furthermore, through the conductivity, they both affect the electric field across the *p* layers as described in the work by Pope *et al.*[14] The electric field is given by

$$E = \frac{J}{ep(T)\mu_p(T)}, \tag{1}$$

where J is the sum of the radiative and nonradiative current densities in the active region, e is the electronic charge, $p(T)$ is the temperature-dependent hole concentration, and $\mu_p(T)$ is the temperature-dependent hole mobility. In the simulation the hole concentration is calculated using the acceptor concentration, the donor concentration, and acceptor ionization energy. As discussed earlier the thermal anneal step (and the temperature used) increases the acceptor concentration, and a compensating donor concentration can be present though this is generally an order of magnitude less than the acceptor concentration.[24–27] The values of the acceptor and compensating donor concentrations and the hole mobility for our samples are not known so we have used values measured on GaN samples with acceptor concentrations of (2, 4, and 8) $\times10^{19}$ cm^{-3}.[24–26] In Table II the values of acceptor concentration, compensating donor concentration, and acceptor ionization energy are given for *p*-GaN, which were determined from the analysis of experimental temperature-dependent Hall measurements[24–26] are given along with the corresponding value of the hole concentration at 300 K.

TABLE II. Values of the acceptor concentration (N_A), donor concentration (N_D), acceptor activation energy (E_A), hole concentration (p), and the hole mobility (μ_p) used in the simulation at 300 K within the *p*-doped layers for the three simulated structures.

p-GaN	$N_A(cm^{-3})$	2×10^{19}	4×10^{19}	8×10^{19}
	$N_D(cm^{-3})$	2×10^{18}	2×10^{18}	5×10^{18}
	E_A(meV)	175	170	160
	$p(cm^{-3})$	5×10^{16}	1.5×10^{17}	8×10^{17}
p-AlGaN	$N_A(cm^{-3})$	3×10^{17}	6×10^{17}	12×10^{17}
	$N_D(cm^{-3})$	3×10^{16}	6×10^{16}	12×10^{16}
	8% Al			
	E_A(meV)	194	194	194
	$p(cm^{-3})$	1.3×10^{16}	1.5×10^{16}	1.7×10^{16}
	30% Al			
	E_A(meV)	260	260	260
	$p(cm^{-3})$	1.7×10^{15}	1.7×10^{15}	1.7×10^{15}
	$\mu_p(cm^2/V\ s)$	15	6	3

We assume that the *p*-AlGaN cladding and electron-blocking layers, shown in Fig. 1, have the same acceptor concentration within each sample and that the donor concentration in AlGaN is 10% of the acceptor concentration which is consistent with measurements by Tanaka *et al.*[27] We also assume that the acceptor concentration increases in a similar manner to *p*-GaN, so that the acceptor concentration in AlGaN rises in proportion to an increasing acceptor concentration in *p*-GaN. However, the value of the acceptor concentration in each case is assumed to be smaller than that in GaN (and the ionization energy is larger—see below) so that a smaller hole concentration (approximately 2×10^{16} cm^{-3}) is produced to be consistent with experimental data.[27,28] The acceptor ionization energy is assumed to increase with Al composition at a rate of 3 meV per percentage of Al (Ref. 29) producing ionization energy values, 194 meV (8%) and 260 meV (30%), which are similar to those in the work by Lee *et al.*;[30] the values for the acceptor concentration, compensating donor concentration, acceptor ionization energy, and hole concentration in AlGaN are given in Table II.

To ensure consistency we have, in addition to using the hole concentration versus reciprocal temperature data of Refs. 24 and 25, also used the hole mobility versus temperature data from the same publication.[24,25] The published measured data show that the presence of increased acceptor and donor concentrations causes the hole mobility to decrease at 300 K, from 15 $cm^2/V\ s$ for an acceptor concentration of 2×10^{19} cm^{-3} to 3 $cm^2/V\ s$ at an acceptor concentration of 8×10^{19} cm^{-3}; the mobility values used for our three samples are given in Table II. In addition the peak hole mobility moves to higher temperatures with increasing acceptor concentrations such that for 2×10^{19} cm^{-3} the peak occurs at ~150 K while for 8×10^{19} cm^{-3} the peak occurs at 350 K.

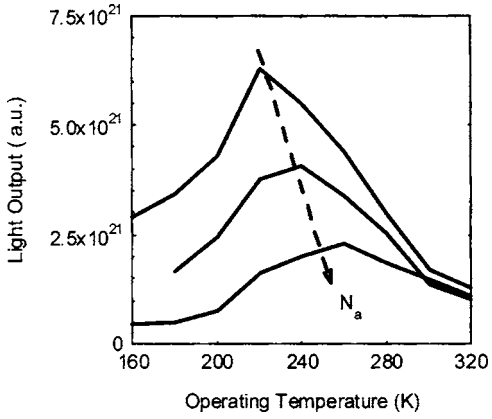

FIG. 5. Simulated light output vs temperature at a fixed current density (25 A cm^{-2}) for samples with acceptor concentrations N_A of (2,4, and 8) $\times 10^{19}$ cm^{-3} in the *p*-GaN layer.

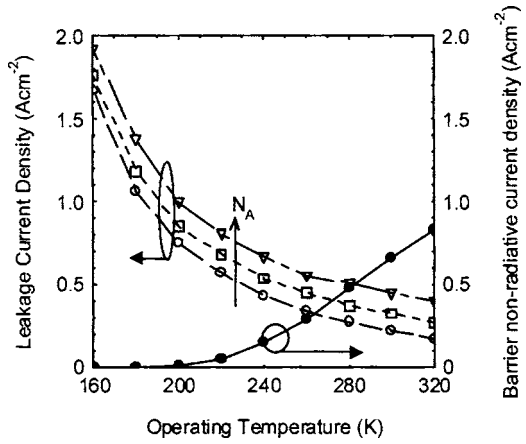

FIG. 6. Simulated current densities of drift leakage for acceptor concentrations N_A of (2,4, and 8)$\times 10^{19}$ cm^{-3} and nonradiative recombination in the barriers for an acceptor concentration of 4×10^{19} cm^{-3}.

For the *p*-AlGaN system there is a lack of published hole mobility data as a function of temperature for different Al compositions, and hence we have assumed that the hole mobility in all the *p* layers is the same within the simulated example. The work by Tanaka *et al.*[27] shows that the hole mobility for AlGaN with 8% Al has similar values to GaN around 300 K and we assume that the temperature dependence is also the same as for GaN.

IV. SIMULATED RESULTS

The simulated light output versus temperature at a fixed current density of 25 A cm^{-2} for the three samples with different activated acceptor concentrations is shown in Fig. 5. The simulated results shown in Fig. 5 reproduce the trends observed experimentally in Fig. 3. A decrease in the light output and a shift of the maximum light output to higher temperatures are observed in the simulated results below 300 K when the activated acceptor concentration is increased and hole mobility is reduced. Above 300 K the simulated data reproduce similar values for the light output for the three different acceptor concentrations. If only the activated acceptor concentration (which changes the hole concentration) in the *p*-GaN layer is changed, which is of course contrary to the published results that also shows a change in the mobility,[24,25] the simulated data do not reproduce the trends observed in the experiment. We conclude that the effect of varying the acceptor and donor concentrations and the hole mobility in our model does reproduce the experimental behavior with anneal temperature.

Through the simulated data we are able to identify the mechanisms that lead to the distinct light output behavior with temperature. At high temperatures the electrons can thermally escape out of the QW; however, the AlGaN electron-blocking layer prevents a substantial fraction of them from being lost from the core of the structure. The initial increase in the light output as the temperature is lowered from 320 K is a result of improved electron confinement in the QWs. By comparing simulations of the structures with and without the AlGaN blocking layer, we determine that the presence of the blocking layer increases the electron population in the QWs near the blocking layer but also increases the electron population in the barriers regions. It is the increased barrier nonradiative recombination (Shockley-Reed-Hall) that leads to a reduced light output even though most of the carriers are not lost from the core of the structure. In Fig. 6 the nonradiative current component within the barrier regions is shown as a function of temperature for a structure with an acceptor concentration of 4×10^{19} cm^{-3}, the other two structures provide similar curves.

We find that electrons are lost from the core of the structure to the *p*-type GaN layer through drift leakage. The electron drift leakage current component as a function of temperature for the three simulated structures is also shown in Fig. 6. The leakage component increases as the temperature is lowered for all the structures and increases when the acceptor concentration is increased and the hole mobility is decreased. Note that the increase in electron leakage current with increasing acceptor concentration occurs because the decrease in hole mobility accompanying the increasing acceptor concentration has a larger effect. The values for the leakage current may seem small, i.e., ~1–2 A cm^{-2}, but when compared to the total current density, 25 A cm^{-2}, the drift leakage is significant. In Fig. 7(a) the simulated conduction-band profiles at operating temperatures of 300, 240, and 180 K for a structure with an acceptor concentration of 4×10^{19} cm^{-3} are shown. At 300 K the *p* side of the structure is slightly tilted due to electric fields that are produced across the *p*-doped layers. Figure 7(b) shows a magnified diagram of the active region and the *p*-AlGaN electron-blocking layer. The electric field across the *p*-AlGaN (labeled A) electron-blocking layer is considerably larger than the fields across the *p*-AlGaN strained layer superlattice (SLS) (labeled B) and *p*-GaN (labeled C) layers. As the temperature is decreased, the electric field across the *p* layers increases due to the decrease of the hole concentration and the temperature-dependent hole mobility as described by Eq. (1), resulting in an increased electron leakage through drift as shown in Fig. 6. Hence, the electron population in the QWs decreases and as a consequence the light output reduces.

Overall the effect of the increased electron confinement in the QWs competes with drift electron leakage to produce the distinct temperature dependence of the light output. Fig-

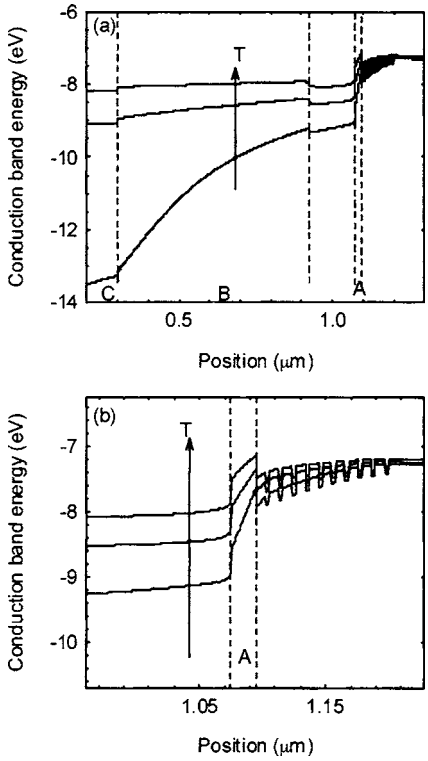

FIG. 7. (a) Simulated conduction-band profile of the active region at 180, 240, and 300 K for a structure with an acceptor concentration of 4×10^{19} cm^{-3} in the *p*-GaN layer; the arrow shows the increase of temperature. The *p*-$Al_{0.30}Ga_{0.70}N$ electron-blocking layer is labeled A, the p-AlGaN SLS is labeled B, and the *p*-GaN cap layer is labeled C. (b) Magnified conduction band of the QWs and *p*-$Al_{0.30}Ga_{0.70}N$ electron-blocking layer.

ure 8 shows the simulated conduction-band profiles at 240 K as we mimic the samples with three different anneal temperatures (which have different acceptor concentrations and mobility in the *p*-doped layers). The electric field across the *p*-AlGaN electron-blocking layer increases by about 10% as the acceptor concentration goes from its lowest to its highest value. However, the electric field across the *p*-AlGaN SLS increases more substantially for the higher acceptor concentration; raising the acceptor concentration from 2×10^{19} to 8×10^{19} cm^{-3} produces an increase of the electric field from 6.5×10^{3} to 1.58×10^{4} V cm^{-1}, an increase of more than a factor of 2 due to the concomitant decrease in hole mobility. The combination of the increasing electric fields across the *p*-AlGaN layers as the acceptor concentration is raised results in the increase of leakage current as shown in Fig. 6. The distinct light output as a function of temperature is therefore due to a competition between the increased electron confinement in the QWs and leakage by drift.

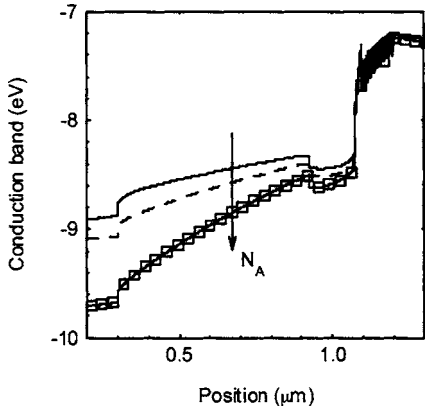

FIG. 8. Simulated conduction-band profiles at 240 K for structures with acceptor concentrations of $(2,4,$ and $8)\times10^{19}$ cm^{-3}; the arrow shows the increase in acceptor concentration N_A.

V. CONCLUSIONS

In conclusion, the light output versus temperature characteristics have been measured for InGaN/GaN QW LEDs which were annealed at different temperatures. All four of the LED samples produce a distinct light output with temperature which increases as the operating temperature is decreased from room temperature, reaches a maximum, and then decreases with subsequent decreases in operating temperature. It is found that an increase of the thermal anneal temperature, which is believed to activate the acceptors in these LEDs, results in a change in the temperature dependence of the light output at a fixed current density. At temperatures below 300 K the light output decreases and the peak light output shifts to higher operating temperatures when the thermal anneal temperature is increased. Through measurement of the absorption and emission spectra it is found that the increased thermal anneal temperature has no effect on the QWs within the structures. The light output versus temperature has been simulated using SIMWINDOWS, and it is found that by changing the concentration of acceptor atoms (and consequentially the concentration of compensating donors and the hole mobility), the trends observed in the experimental results can be reproduced. At operating temperatures around room temperature it is found that nonradiative recombination in the barrier regions is significant as electrons can thermally escape from the wells but are prevented from being lost to the contact by the AlGaN blocking layer and hence populate the barriers. When the operating temperature is decreased the thermal escape of the electrons from the quantum well reduces, but it is found that the electric fields across the *p*-doped layers increase which results in increased drift leakage. Additionally when the acceptor concentration is raised, drift leakage increases due to larger electric fields across the *p*-doped layers due to the concomitant change in hole mobility. The combination of the nonradiative recombination and the drift leakage combine to produce the distinct temperature behavior of the light output. Therefore, it can be concluded that the experimental observations can be attributed to changes of the acceptor concentration and mobility in the *p* layers when the thermal anneal temperature is changed.

[1]W. Gotz, N. M. Johnson, D. P. Bour, M. D. McCluskey, and E. E. Haller, Appl. Phys. Lett. **69**, 3725 (1996).
[2]H. Amano, M. Kito, K. Hiramatsu, and I. Akasaki, Jpn. J. Appl. Phys., Part 2 **28**, L2112 (1989).
[3]S. Nakamura, T Mukai, M. Senoh, and N. Iwasa, Jpn. J. Appl. Phys., Part 2 **31**, L139 (1992).
[4]W. Gotz, N. M. Johnson, J. Walker, D. P. Bour, and R. A. Street, Appl. Phys. Lett. **68**, 667 (1996).
[5]M. G. Cheong, K. S. Kim, C. S. Kim, R. J. Choi, H. S. Yoon, N. W. Namgung, E.-K. Suh, and H. J. Lee, Appl. Phys. Lett. **80**, 1001 (2002).
[6]S. H. Chung, M. Lachab, T. Wang, Y. Lacroix, D. Basak, Q. Fareed, Y.

Kawakami, K. Nishino, and S. Sakai, Jpn. J. Appl. Phys., Part 1 **39**, 4749 (2000).
[7]Y. C. Cheng *et al.*, Jpn. J. Appl. Phys., Part 1 **40**, 2143 (2001).
[8]J. Neugebauer and C. G. Van de Walle, Phys. Rev. Lett. **75**, 4452 (1995); Appl. Phys. Lett. **68**, 1829 (1996).
[9]C. G. Van de Walle, C. Stampfl, and J. Neugebauer, J. Cryst. Growth **189/190**, 505 (1998).
[10]M. E. Lin, G. Xue, G. L. Zhou, J. E. Greene, and H. Morkoc, Appl. Phys. Lett. **63**, 932 (1993).
[11]SIMWINDOWS, http://www.ocs.colorado.edu/SimWindows/simwin.html
[12]D. Lancefield, A. Crawford, B. Beaumont, P. Gibart, M. Heuken, and M. Di Forte-Poisson, Mater. Sci. Eng., B **B82**, 241 (2001).
[13]A. Hori, D. Yasunga, A. Satake, and K. Fujiwara, Appl. Phys. Lett. **79**, 3723 (2001).
[14]I. A. Pope, P. M. Smowton, P. Blood, J. D. Thomson, M. J. Kappers, and C. J. Humphreys, Appl. Phys. Lett. **82**, 2755 (2003).
[15]C. J. Youn, T. S. Jeong, M. S. Han, J. W. Yang, K. Y. Lim, and H. W. Yu, J. Cryst. Growth **250**, 331 (2003).
[16]P. Blood, J. Appl. Phys. **58**, 2285 (1985); P. M. Smowton, P. Blood, P. C. Mogensen, and D. P. Bour, Int. J. Optoelectron. **10**, 383 (1996).
[17]M. D. McCluskey, L. T. Romano, B. S. Krusor, N. M. Johnson, T. Suski, and J. Jun, Appl. Phys. Lett. **73**, 1281 (1998).
[18]C.-C. Chuo, C.-M. Lee, and J.-I. Chyi, Appl. Phys. Lett. **78**, 314 (2001).
[19]Y.-C. Chang, S. Jursenas, S.-W. Feng, C. C. Yang, C.-T. Kuo, and J.-S. Tsang, Phys. Status Solidi A **201**, 221 (2004).
[20]H. Sakuta, Y. Kawano, Y. Yamanaka, S. Kurai, and T. Taguchi, Phys. Status Solidi C **7**, 2407 (2005).
[21]M. D. McCluskey, L. T. Romano, B. S. Krusor, D. Hofstetter, D. P. Bour, M. Kneissl, N. M. Johnson, T. Suski, and J. Jun, MRS Internet J. Nitride Semicond. Res. **4S1**, G3.42 (1999).
[22]J. D. Thomson, I. H. Brown, P. M. Smowton, P. Blood, W. W. Chow, A. M. Fox, and S. M. O. Izquierdo, Proc. SPIE **5722**, 392 (2005).
[23]D. W. Winston and R. E. Hayes, IEEE J. Quantum Electron. **34**, 707 (1998).
[24]W. Gotz and N. M. Johnson, in *Gallium Nitride (GaN) II*, edited by J. I. Pankove and T. D. Moustakas (Academic, New York, 1998), p. 192.
[25]D. Steigerwald, S. Rudaz, H. Liu, R. S. Kern, W. Gotz, and R. Fletcher, JOM **49**, 18 (1997).
[26]H. Morkoc, in *Nitride Semiconductors and Devices*, Springer Series in Materials Science Vol. 32, edited by R. Hull, R. M. J. Osgood, J. Parisi, and H. Vuarli Mont (Springer Berlin, 1999), p. 258.
[27]T. Tanaka, A. Wantanbe, H. Amano, Y. Kobayashi, I. Akasaki, S. Yamazaki, and M. Koike, Appl. Phys. Lett. **65**, 593 (1994).
[28]M. Suzuki, J. Nishio, M. Onomura, and C. Hongo, J. Cryst. Growth **189/190**, 511 (1998).
[29]J. Piprek and S. Nakamura, IEE Proc.: Optoelectron. **149**, 145 (2002).
[30]S.-N. Lee *et al.*, J. Cryst. Growth **272**, 455 (2004).